BIOCHEMISTRY
including biophysical chemistry & molecular biology

Article

pubs.acs.org/biochemistry

Tuning a Polar Molecule for Selective Cytoplasmic Delivery by a pH (Low) Insertion Peptide

Dayanjali Wijesinghe,[†] Donald M. Engelman,[‡] Oleg A. Andreev,[†] and Yana K. Reshetnyak*,[†]

[†]Physics Department, University of Rhode Island, 2 Lippitt Road, Kingston, Rhode Island 02881, United States

[‡]Department of Molecular Biophysics and Biochemistry, Yale University, P.O. Box 208114, New Haven, Connecticut 06520, United States

ABSTRACT: Drug molecules are typically hydrophobic and small in order to traverse membranes to reach cytoplasmic targets, but we have discovered that more polar molecules can be delivered across membranes using water-soluble, moderately hydrophobic membrane peptides of the pHLIP (pH low insertion peptide) family. Delivery of polar cargo molecules could expand the chemical landscape for pharmacological agents that have useful activity but are too polar by normal drug criteria. The spontaneous insertion and folding of the pHLIP peptide across a lipid bilayer seeks a free energy minimum, and insertion is accompanied by a release of energy that can be used to translocate cell-impermeable cargo molecules. In this study, we report our first attempt to tune the hydrophobicity of a polar cargo, phallacidin, in a systematic manner. We present the design, synthesis, and characterization of three phallacidin cargoes, where the hydrophobicity of the cargo was tuned by the attachment of diamines of various lengths of hydrophobic chains. The phallacidin cargoes were conjugated to pHLIP and shown to selectively inhibit the proliferation of cancer cells in a concentration-dependent manner at low pH.

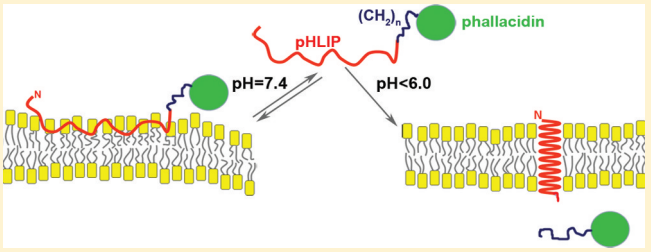

Targeted drug delivery would allow drugs to preferentially affect diseased cells, enhancing therapeutic efficacy while reducing side effects. Targeting could be particularly important for cancer therapy, because most anticancer drugs are toxic, not only killing cancer cells but also causing serious damage to healthy tissues. Despite significant progress toward drugs that specifically target protein biomarkers for certain kinds of cancer cells, there is still no "silver bullet" against cancer. One reason for the limited success so far is that cells in tumors are heterogeneous and selection for resistance to protein-targeted drugs and to the immune system can occur.[1] An alternative might be to find a targeting mechanism that does not depend on a selectable marker. One of the universal differences between cancerous and normal tissues is that the former exhibit a significantly acidic extracellular environment. Acidosis is a hallmark of solid tumor development at both very early and advanced stages, as a consequence of anaerobic metabolism (the Pasteur effect)[2] and "aerobic glycolysis", known as the Warburg effect.[3]

To target acidic tissues, we have developed a new approach, based on the action of a water-soluble, moderately hydrophobic membrane polypeptide, pHLIP (pH low insertion peptide), derived from the bacteriorhodopsin C helix. pHLIP is a soluble peptide that was found to fold and insert across a membrane to form a stable transmembrane α-helix under acidic conditions.[4] When triggered by low pH, members of the pHLIP peptide family act as monomeric, membrane-inserting peptides that translocate their carboxyl termini across membranes into the cytoplasms of targeted cells, while the amino termini remain in the extracellular space, moving the peptide across the plasma membrane lipid bilayers.[5] Because the insertion occurs at low pH, acidic tissues are targeted, so pHLIP has a dual delivery capability: it can tether N-terminally linked cargo molecules to the surfaces of cells in diseased tissues and can move a C-terminally linked, cell-impermeable cargo molecule across the membrane into the cytoplasm using the free energy of insertion and folding.[6,7] Use of a cleavable link, such as a disulfide, releases the cargo inside the cell.[8,9] Low pH leads to the protonation of negatively charged residues (Asp or Glu), which enhances peptide hydrophobicity, increasing the affinity of the peptide for the lipid bilayer and triggering peptide folding and subsequent membrane insertion.[10−12] The source of energy for moving polar molecules attached to pHLIP through the hydrophobic layer of a membrane is the membrane-associated folding of the polypeptide.[13−15] The affinity of a peptide for a membrane at low pH is ∼5 times higher than at high pH, allowing pHLIP to distinguish and mark acidic diseased tissue[10,16,17] associated with various pathological states, such as cancerous tumors, inflammation, ischemia, stroke, etc.

Our recent findings indicate that pHLIP facilitates the translocation of phalloidin, a cell-impermeable polar toxin, which leads to the inhibition of the proliferation of cancer cells in a pH-dependent fashion.[8] However, the antiproliferative effect was observed only when a hydrophobic facilitator (rhodamine) was attached to the peptide inserting end. An

Received: June 24, 2011
Revised: October 25, 2011
Published: October 26, 2011

alternative approach is to modify the properties of the cargo molecule to optimize delivery, and the goal of this study is to tune properties of the pHLIP−cargo constructs to achieve the most efficient pH-dependent translocation of cargo molecules across the lipid bilayer. The properties of a molecule delivered into cells will help to define the chemical landscape available for the use of pHLIP. Here we present the design, synthesis, and characterization of three phallacidin cargoes, where the hydrophobicity of the cargo was tuned by attachment of diamines having various lengths of hydrophobic chains. Three constructs in which pHLIP was linked to phallacidin cargoes of different polarity were synthesized and characterized, and the antiproliferative effect was tested on cultured cells.

MATERIALS AND METHODS

Peptide Preparation. The pHLIP peptide (AEQNPIYWARYADWLFTTPLLLLDLALLVDADEGCT) was prepared by solid phase peptide synthesis at the W. M. Keck Foundation Biotechnology Resource Laboratory at Yale University. The lyophilized powder was soluble in 3 M urea or DMSO (dimethyl sulfoxide). When dissolved in urea, the peptide was transferred to buffer using a G-10 size-exclusion spin column. The concentration of the peptide was determined spectrophotometrically by measuring the absorbance at 280 nm (ε_{280} = 13940 M^{-1} cm^{-1}).

Synthesis of Phallacidin-$(CH_2)_n$SH. *Materials.* Phallacidin was purchased from GenoLite Biotek. *N*-Hydroxysuccinimide (NHS), *N*,*N*′-dicyclohexylcarbodiimide (DCC), and *N*-succinimidyl 3-(2-pyridyldithio)propionate (SPDP) were from Thermo Scientific. Hexamethylenediamine (98%), 1,4-diaminobutane (99%), and 1,10-diaminodecane (97%) were from Sigma Aldrich.

Step 1. Phallacidin (2.6 mg, 3.10 μmol) was dissolved in 100 μL of dry DMF (dimethylformamide) and transferred into a 1.5 mL glass vial followed by addition of NHS (2.5 mg, 21.6 μmol, 7 equiv) in 30 μL of dry DMF and mixed well. DCC (1.15 mg, 5.57 μmol, 1.8 equiv) was added to the reaction mixture. The reaction mixture was stirred at room temperature overnight, centrifuged, and separated from the urea crystals. The progress of the reaction was monitored by reverse phase HPLC (high-performance liquid chromatography) at 0 and 12 h [Agilent Technologies Zorbax SB-C18, 4.6 mm × 250 mm column; flow rate of 1 mL/min; phase A of water and 0.05% TFA (trifluoroacetic acid); phase B of acetonitrile and 0.05% TFA; 30 min gradient from 95:5 A:B to 50:50 A:B]. The phallacidin starting material elutes at 24.9 min, while activated hydroxysuccinimidephallacidin elutes at 23.6 min. The reaction was completed by 12 h.

Step 2. The supernatant from step 1, which contained the activated hydroxysuccinimidephallacidin, was added to diamines $H_2N(CH_2)_nNH_2$ (n = 4, 6, or 10) dissolved in dry DMF (31 μmol, 10 equiv of phallacidin), and the reaction mixture was stirred at room temperature for 10 h. The addition of the diamine resulted in the formation of a precipitate, dehydrated phallacidin diamine salt. The product, phallacidin-$(CH_2)_nNH_2$ (phallCn) was found both in the precipitate and in the supernatant. The precipitate was separated by centrifugation and dissolved in 120 μL of a MeOH/H_2O mixture (1:1). The product was purified using HPLC and lyophilized. The elution times of phallacidin-$(CH_2)_4NH_2$ (phallC4), phallacidin-$(CH_2)_6NH_2$ (phallC6), and phallacidin-$(CH_2)_{10}NH_2$ (phallC10) were 23.1, 24.6, and 29.5 min, respectively, as expected from the increasing hydrophobicities. The lyophilized powder was then dissolved in 100 μL of a MeOH/H_2O mixture (1:1), quantified by measurement of the OD (optical density) at 300 nm (ε_{300} of phallacidin equals 10100 M^{-1} cm^{-1}), and analyzed using ESI (electrospray ionization) mass spectrometry. The molecular masses of the phallotoxins phallC4, phallC6, and phallC10 were 917.23, 945.18, and 1001.22 Da, respectively (the expected molecular masses were 917.06, 945.12, and 1001.23 Da, respectively).

Step 3. The products from step 2 [in 100 μL of a MeOH/water mixture (1:1)] were transferred into 200 μL of 100 mM phosphate buffer (pH 8). A solution of SPDP (starting from 5 equiv of phallCn) in DMSO was added to the reaction mixture and stirred at room temperature. After ∼2 h, most of the SPDP was hydrolyzed to PDP and no further formation of phallCn-PDP was observed. The pH of the reaction mixture was adjusted to pH 8, and more SPDP was added until almost all phallCn was reacted. The progress of the reaction was monitored using HPLC. Phallacidin-$(CH_2)_n$SH (phallCnSH) was obtained by reducing the disulfide bond in the phallCn-PDP using TCEP (20 equiv of SPDP added) in 100 mM phosphate buffer (pH 8) for 30 min, purified using reverse phase C18 HPLC, lyophilized, and characterized using ESI mass spectrometry. The elution times and molecular masses of phallotoxins on HPLC runs with 30 min gradients from 99:1 A:B to 70:30 A:B (flow rate of 1 mL/min) were 30.3 min and 846.15 Da for phallacidin, 32.4 min and 1005.17 Da for phallC_4SH, 35.5 min and 1033.03 Da for phallC_6SH, and 44.4 min and 1089.07 Da for phallC_{10}SH, respectively.

Synthesis of pHLIP-S-S-$(CH_2)_n$-phallacidin. The lyophilized phallC_n-PDPs were dissolved in DMSO to a concentration of ∼5 mM, followed by the addition of pHLIP peptide (2 equiv) dissolved in DMSO, and incubated at room temperature. More pHLIP was added if needed until almost all phallC_n-PDPs were reacted. The progress of the reaction was monitored using HPLC (flow rate of 1 mL/min; 60 min gradient from 99:1 A:B to 5:95 A:B). pHLIP-$C_n$phall was analyzed using SELDI-TOF (surface-enhanced laser desorption ionization time-of-flight) mass spectrometry and quantified by measurement of the OD at 280 and 300 nm (ε_{280} and ε_{300} of 13940 and 2999 M^{-1} cm^{-1} for pHLIP and ε_{280} and ε_{300} of 10944 and 10100 M^{-1} cm^{-1} for phallacidin, respectively).

Measurements of the Water−Octanol Partition Coefficient. The polarities of the phallotoxin cargoes were determined by the assessment of relative partitioning between aqueous and octanol liquid phases. Constructs dissolved in a 1:1 MeOH/water mixture were added to 0.5 mL of 10 mM phosphate buffer (pH 5.5) (saturated with argon) to concentrations of 20 and 30 μM, followed by the addition of argon-saturated *n*-octanol (0.5 mL), and sealed under argon. The solutions were mixed by rotation for 24 h at room temperature and left for an additional 24−48 h to reach equilibrium. After phase separation, absorption at 300 nm was recorded. The molar extinction coefficients in *n*-octanol and phosphate buffer are assumed to be the same, and the ratio of the OD readings was used directly to calculate the partition coefficient (P = $OD_{n\text{-octanol}}/OD_{water}$) and log P values. A fraction of the aqueous solution was analyzed using HPLC to ensure that no dimers of the phallotoxin were formed.

Liposome Preparations. Liposomes were prepared by extrusion. POPC (1-palmitoyl-2-oleoyl-*sn*-glycero-3-phosphocholine) (500 μL of a 10 mg/mL solution in chloroform) was transferred to a 100 mL round-bottom flask, and a lipid layer was obtained by evaporating the choloroform in a rotary

evaporator, followed by drying under high vacuum for 2 h. The lipid layer was resuspended in 10 mM phosphate buffer (pH 8) and extruded 31 times through a 50 nm membrane, yielding large unilamellar vesicles.

Measurements of Intrinsic Peptide Fluorescence and Circular Dichroism (CD) Spectroscopic Signals. Intrinsic peptide fluorescence and circular dichroism (CD) spectra were recorded on a PC1 ISS spectrofluorometer (ISS, Inc.) and a MOS-450 spectrometer (Bioligic, Inc.), respectively, while the temperature was controlled. All measurements were performed at 25 °C. Samples of 7 μM pHLIP-C$_n$phall incubated with 1.5 mM POPC or in buffer (pH 8) overnight were used for the measurements of CD and fluorescence signals of the three states. pHLIP-C$_n$phall (4 μM, pH 8) incubated overnight was used for the aggregation of the peptide and cargo in aqueous medium. Peptide fluorescence spectra were recorded from 310 to 400 nm using excitation wavelengths of 280 nm. Peptide CD spectra were recorded from 190 to 260 nm at 0.5 nm increments using a sample cuvette with an optical path length of 0.5 cm.

Binding Assay. *Materials and Preparation of Stock Solutions.* Rabbit muscle actin was purchased from Cytoskeleton Inc. To obtain polymerized filamentous actin (F-actin), we dissolved the monomeric globular actin (G-actin) in 100 μL of water and incubated the mixture for 1 h at room temperature. After centrifugation at 13000*g* for ~15 min, the amount of G-actin in the supernatant was quantified by measuring the OD at 290 nm (the ε_{290} of G-actin is 26600 M^{-1} cm^{-1}). G-Actin was diluted to 3.5 mg/mL in 2 mM phosphate buffer (pH 8) supplemented with 0.2 mM $CaCl_2$ and 0.2 mM ATP and incubated for 1 h at 4 °C. Polymerization was induced by addition of 50 mM KCl, 2 mM $MgCl_2$, and 1 mM ATP and incubation for 1 h at room temperature. Texas Red-X phalloidin (phallTxR) was purchased from Invitrogen Corp. phallTxR was dissolved in DMF and quantified by measuring the OD at 583 nm (ε_{583} of phallTx in MeOH of 95000 M^{-1} cm^{-1}). Previously prepared and lyophilized phallotoxins (phallacidin, phallC4SH, phallC6SH, and phallC10SH) were dissolved in DMSO and quantified by measuring the OD at 300 nm (ε_{300} of phallotoxins of 10100 M^{-1} cm^{-1}).

Assay of Binding of phallTxR to Actin. Samples of 0.6 μM phallTxR with different F-actin concentrations (from 0 to 6.6 μM) were prepared in polymerizing buffer [2 mM phosphate buffer (pH 8) containing 50 mM KCl, 2 mM $MgCl_2$, 0.2 mM $CaCl_2$, and 1 mM ATP] and incubated for 2 h at room temperature. The fluorescence anisotropy and intensity of each sample were measured with excitation and emission at 570 and 610 nm, respectively, while the temperature was controlled.

Competition Binding Assay. The assay is based on titration of 0.3 μM phallTxR and 0.3 μM phallotoxin by increasing concentrations of F-actin; 10× TCEP was added to a 60 μM stock solution of phallotoxins in polymerizing buffer and incubated for 10 min to reduce the disulfide bond. Samples of 0.3 μM phallTxR and each phallotoxin at 0.3 μM were prepared in polymerizing buffer followed by mixing with F-actin, which yielded final F-actin concentrations of 0, 0.3, 0.6, 1.2, and 2.4 μM in each sample, and incubated overnight at 4 °C. The fluorescence anisotropy of each sample was measured with excitation and emission at 570 and 610 nm, respectively, measured using the PC1 spectrofluorometer while the temperature was controlled.

Cell Line. Human cervical adenocarcinoma HeLa cells were purchased from the American Tissue and Culture Collection (ATCC). HeLa cells were propagated in DMEM (Dulbecco's modified Eagle's medium) [with 4.5 g/L D-glucose and 40 mg/L sodium pyruvate (Gibco)] supplemented with 10% FBS (fetal bovine serum) (Gibco) and ciprofloxacin hydrochloride (1 μg/mL) (from Cellgro, Voigt Global Distribution) in a humidified atmosphere of 5% CO_2 at 37 °C. HeLa cells were adapted to pH 6.2 by propagation in pH 6.2 DMEM supplemented with 10% FBS and ciprofloxacin hydrochloride (1 μg/mL) in a humidified atmosphere of 5% CO_2 at 37 °C.

Proliferation Assay. Stock solutions of phallacidin, phalloidin-oleate, phallC$_n$SH, and pHLIP-C$_n$phall were prepared in DMSO at 400 μM. A human cervix adenocarcinoma cell line (HeLa) obtained from the ATCC was grown at pH 6.2 and 7.4. HeLa cells were seeded in 96-well plates (Costar) at densities of 4000 and 2000 cells/well for treatment on the following day. A DMSO stock of constructs was diluted with sterile Leibovitz's L-15 phenol free medium (L-15) at pH 6.0 or 7.4 to give treatment solutions in the 0–6 μM range. Appropriate amounts of DMSO were added to ensure that all treatment samples contained the same amount of DMSO by volume (1.5%). After removal of cell media, the L-15 treatment solutions at pH 6.0 or 7.4 (95 μL) were added to cells grown at pH 6.2 or 7.4, respectively, and then the plate was incubated at 37 °C for 3 h. After treatment, 200 μL of DMEM at pH 6.2 or 7.4 was added to the corresponding wells and 10 μL of FBS to each well to provide 10% FBS in cell medium before the plate was returned to the incubator. The cell density of the "0 μM, pH 6.2" and "0 μM, pH 7.4" controls usually reached 80–90% saturation in the well after they had grown for 4–6 days. The viable cell number was quantified using the MTS reagent (Promega CellTiter 96 AQueous One Solution Cell Proliferation Assay). OD values at 490 nm were obtained using a plate reader (iMark Microplate reader from Bio-Rad). Because the rate of cell growth is slightly different at low and neutral pH values, all numbers were normalized to 100% using wells in which no construct was added to the media at various pH values.

RESULTS

Design and Synthesis of Phallacidin Cargoes with Different Hydrophobicities. The major goals of our work are to systematically vary the hydrophobicity of a polar cargo, phallatoxin, and to investigate pHLIP-mediated pH-dependent cellular delivery of constructs of cargoes with different polarities. We chose phallacidin (Figure 1), which is a cyclic

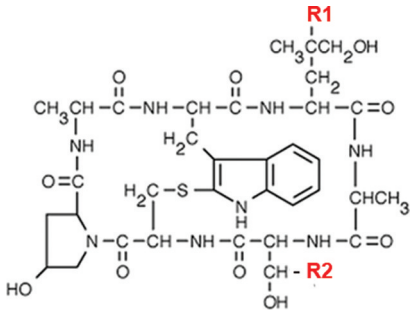

Figure 1. Chemical structures of cyclic peptides phalloidin (where R1 = OH and R2 = CH_3), phallodin-rhodamine (where R1 = rhodamine), and phallacidin (where R1 = H and R2 = COOH). Diamines consisting of carbon chains of different lengths [$(CH_2)_4$, $(CH_2)_6$, and $(CH_2)_{10}$] were attached to the COOH group (R2).

cell-impermeable toxin similar to phalloidin that binds to F-actin with high affinity.[18,19] Phallacidin has a free COOH group suitable for conjugation purposes, and we tuned the hydrophobicity of the phallacidin cargo by reacting it with diamines $NH_2(CH_2)_nNH_2$ with different hydrophobic chain lengths [$(CH_2)_n$, where n could vary from 2 to 12 carbon atoms]. We had already tested commercially available phalloidin oleate, with 15 carbon atoms, which has a log P value of 1.7, and observed 60, 70, and 95% inhibition of proliferation of HeLa cells after treatment of cells with 1, 2, and 4 μM phalloidin oleate, respectively (data not shown), which indicate that attachment of 15 carbon atoms to phalloidin makes it too hydrophobic, so it can easily cross the lipid bilayer itself. We selected three different lengths of hydrophobic chain diamines, where n is 4, 6, and 10. The phallacidin was conjugated to the various length diamines after converting phallacidin to hydroxysuccinimidephallacidin. We synthesized three phallacidin cargoes with four (phallC4), six (phallC6), and ten (phallC10) carbon atoms. The protocol was adjusted until optimal conditions were established, and the details of the final protocol are given in Materials and Methods. The products were purified using reverse phase C18 HPLC, lyophilized, and characterized by ESI mass spectrometry. The molecular masses obtained for phallacidin cargoes were 917.2 Da for phallC4, 945.2 Da for phallC6, and 1001.2 Da for phallC10 and were very close to the expected values (917.1, 945.1, and 1001.2 Da, respectively).

Characterization of Phallacidin Cargoes with Different Hydrophobicities. To investigate the properties of cargo molecules, we reacted them with the SPDP cross-linker, reduced the S−S bond with TCEP, and purified and characterized the reduced cargoes (see Table 1). The cargo hydrophobicities were evaluated by measuring the logarithm of the octanol−water partition coefficient P, calculated on the basis of the amount of constructs distributed upon equilibration between octanol and water phases, measured by the ODs of phallacidin constructs at 300 nm. The log P values of phallacidin and cargoes are listed in Table 1. Phallacidin with a long chain FA of 10 carbon atoms is preferably distributed into octanol, being hydrophobic, and shows a positive log P of 1.28. Such molecules are expected to cross cellular membranes by themselves (at least at high concentrations), the hydrophobicity being in the range of those of conventional drugs. The polarity of phallC6SH with a log P of −0.09 was very close to the polarity of phalloidin-rhodamine, which has a log P of −0.05 measured previously.[20] Phallacidin with four carbon atoms, as expected, was the most polar of the modified phallacidin cargoes.

Table 1. Characterization of Phallacidin and phallC4, -C6, and -C10 Cargoes[a]

	% acetonitrile	log P
phallacidin	20.3	−1.6
phallC4SH	22.4	−0.74
phallC6SH	25.5	−0.09
phallC10SH	34.4	1.28

[a]Percentages of acetonitrile of cargo elutions from the column and logarithms of the octanol−water partition coefficients (log P).

According to the literature,[18,21,22] it was expected that modification of the COOH group of phallacidin should not affect F-actin binding properties. Phallatoxin binds between actin monomers in filamentous actin and prevents depolymerization.[19,21] We used a fluorescence anisotropy titration assay, in which phalloidin conjugated to the Texas Red (TxR) fluorescent dye was in competition with phallacidin and cargoes for F-actin binding. The assay is based on the increase in the anisotropy of phallTxR when it binds to F-actin. Samples with equal concentrations (0.3 μM) of phallTxR and phallacidin cargoes were prepared with increasing concentrations of F-actin. The samples were incubated overnight, and the fluorescence anisotropy of each sample was measured at a wavelength of 610 nm with excitation at 570 nm (Figure 2).

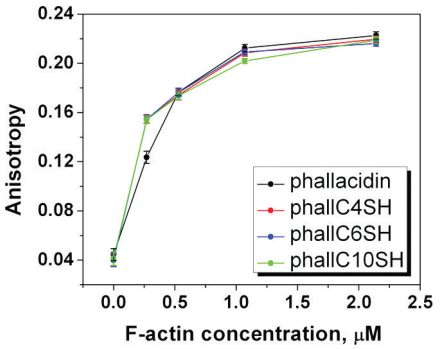

Figure 2. Binding competition assay. Changes in the fluorescence anisotropy of Texas Red conjugated to phalloidin (0.3 μM) were monitored in the presence of phallacidin or phallacidin cargoes (0.3 μM) at different F-actin concentrations.

The anisotropy increases from 0.04 (for unbound phallTxR) to 0.24 when all phallTxR is completely bound (the value of 0.24 was obtained in a separate titration experiment with phallTxR and F-actin in the absence of phallacidin or phallacidin cargoes). Our experiments demonstrate that the anisotropy in the presence of phallacidin cargoes changes in the same way as the anisotropy in the presence of phallacidin, confirming that the attachment of hydrophobic tails to the phallacidin does not alter the affinity for F-actin.

Synthesis and Characterization of pHLIP-C$_n$phall. We synthesized pHLIP-C4phall, pHLIP-C6phall, and pHLIP-C10phall constructs, purified them, performed spectroscopic characterization, and tested their antiproliferative properties. phallC_n-PDP was conjugated with a single Cys residue at the C-terminus of pHLIP to form a S−S bond. The products were purified using reverse phase C18 HPLC, lyophilized, and characterized by SELDI-TOF mass spectrometry (molecular masses of the pHLIP-C4phall, pHLIP-C6phall, and pHLIP-C10phall of 5120.1, 5155.4, and 5204.2 Da, respectively) and quantified by measureement of the OD at 280 and 300 nm.

We have demonstrated previously that changes in intrinsic fluorescence and CD of pHLIP in the presence of liposomes resulting from pH changes are indicative of insertion of the peptide into the lipid bilayer.[4,5] Here, we conducted spectroscopic characterization of pHLIP-C$_n$phall constructs (Figure 3). We found that all constructs are predominantly unstructured in aqueous solution at pH 8, while the position of the fluorescence maximum is slightly shifted to short wavelengths when cargo with a longer carbon chain is conjugated to pHLIP (Table 2). The shift in the position of the maximum is accompanied by the increase in ellipticity at 222 nm. All spectroscopic data indicate that pHLIP-C10phall most probably is more aggregated than pHLIP, pHLIP-C4phall, and pHLIP-C6phall. More pronounced differences between

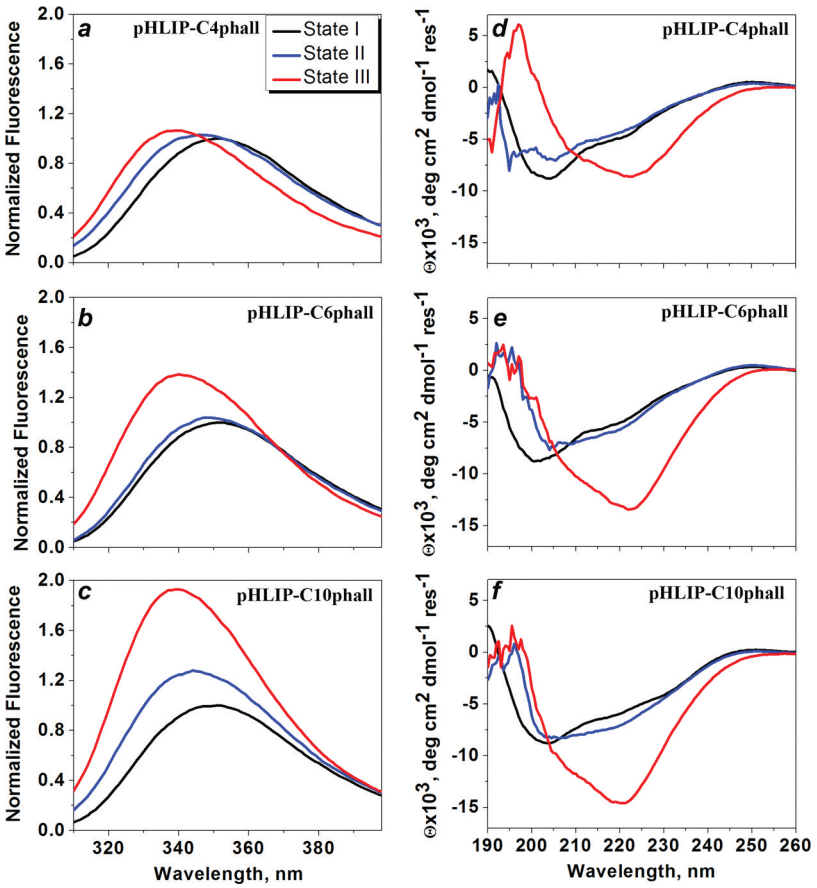

Figure 3. Changes in intrinsic fluorescence (a–c) and CD (d–f) spectral signals upon interaction of pHLIP-C4phall, pHLIP-C6phall, and pHLIP-C10phall with POPC liposomes at various pH values. Black lines represent spectra for the construct in aqueous solution at pH 8, blue lines those upon incubation with POPC liposomes at pH 8, and red lines those after the pH was decreased from 8 to 4.

Table 2. Spectral Parameters of pHLIP-C4phall, pHLIP-C6phall, and pHLIP-C10phall in States I–III[a]

		state I	state II	state III
pHLIP-C4phall	λ_{max} (nm)	350.9	346.6	339.7
	S	1.0	1.08	1.05
	θ_{222}	−4.6	−4.1	−6.05
pHLIP-C6phall	λ_{max} (nm)	349.9	348.3	340.2
	S	1.0	1.03	1.31
	θ_{222}	−4.6	−5.2	−13.4
pHLIP-C10phall	λ_{max} (nm)	349.6	344.6	339.2
	S	1.0	1.28	1.82
	θ_{222}	−5.9	−7.0	−14.6

[a]The parameters were obtained as a result of the analysis of the fluorescence and CD spectra shown in Figure 3: the maximum position of the fluorescence spectrum (λ_{max}), the normalized area under the spectra (S) (normalization was done on the area under the spectrum in state I), and the molar ellipticity at 222 nm (θ_{222}, $\times 10^3$ degrees square centimeters per decimole per residue).

constructs were observed at pH 8 in the presence of POPC. The largest amount of helical structure and the deepest partition of the emitting residues into the core of the bilayer were observed for pHLIP-C10phall. The decrease in pH from 8 to 4 induced a further increase in helical content and partition of the constructs into the membrane accompanied by an increase of fluorescence and a shift of the emission to the short wavelengths. The pH-induced fluorescence and CD changes seen for different constructs in the presence of a lipid bilayer were very similar to those observed for pHLIP alone. These changes were more significant for pHLIP-C10phall than for pHLIP-C4phall. Thus, we concluded that conjugation of phallC_n cargoes, in general, does not affect the pH-dependent ability of pHLIP to interact with the membrane lipid bilayer.

Antiproliferative Effect of pHLIP-$C_n$phall. Finally, we tested the antiproliferative capability of the pHLIP-$C_n$phall constructs. HeLa cells were adapted for low-pH growth (pH 6.2). Cells grown at low and normal (7.4) pH values were treated with increasing concentrations of pHLIP-$C_n$phall, phallC_n, and phallacidin in L-15 phenol free medium at pH 6.0 and 7.4 for 3 h. After treatment, DMEM supplemented with 10% FBS at pH 6.2 or 7.4 was added to the corresponding cells. When the cell density in the control wells (treated with medium) reached 80–90% saturation (after growth for 4–6 days), the number of viable cells was quantified using the MTS reagent. Because the rate of cell growth is slightly different at low and neutral pH values, all numbers were normalized to be 100% where no construct was added to the media. Phallacidin and phallC_n cargoes do not demonstrate an antiproliferative effect at either pH (data not shown). At the same time, the data clearly demonstrate that pHLIP-C4phall and pHLIP-C6phall exhibit concentration-dependent antiproliferative effects only at low pH, while at neutral pH, no effect was observed (Figure 4). At 2 μM pHLIP-C4phall and pHLIP-C6phall, ~30 and ~70%, respectively, of cell death was observed at low pH. As we expected, the increase in cargo hydrophobicity correlates with

dx.doi.org/10.1021/bi2009773 | *Biochemistry* 2011, 50, 10215–10222

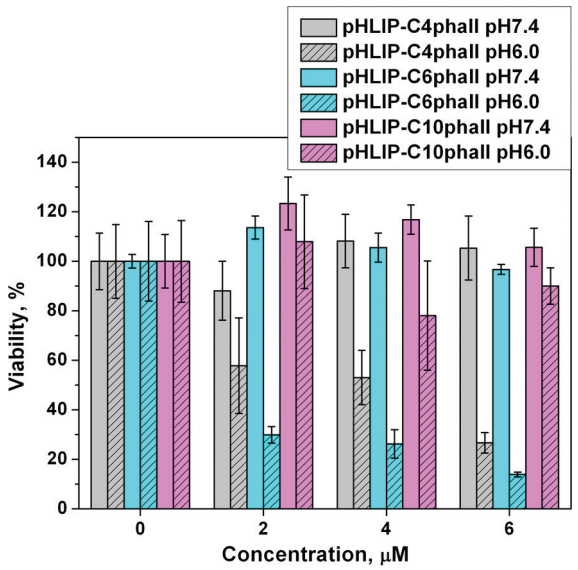

Figure 4. Inhibition of cell proliferation by pHLIP-C4phall, pHLIP-C6phall, and pHLIP-C10phall at low pH.

the enhancement of the antiproliferative effect. However, surprisingly, we did not observe the expected biological effect, when cells were treated with pHLIP-C10phall.

Conformational States of pHLIP-C10phall in Solution at Different pH Values. Because we treated cells with constructs at pH 5.9–6.0 for 3 h, the constructs were dissolved in media at low pH. Previously, we demonstrated that pHLIP has a tendency to aggregate in solution, when the pH is decreased from 8–7.4 to 4–3.[5] When various cargoes are attached to the peptide, the overall hydrophobicity is altered and the solubility also could be changed. The overall hydrophobicity of pHLIP-C10phall is higher than the hydrophobicity of pHLIP-C4phall; therefore, the tendency to aggregate is stronger for pHLIP-C10phall. We compared fluorescence and CD signals of pHLIP-C10phall in aqueous solution at pH 8, 7.4, and 5.9 (Figure 5). The decrease in pH in the range of 6–8 leads to the conformational changes accompanied by the shift of the position of maximal fluorescence from 349 to 346 nm, the increase in the amount of helical structure, and the reduction of the quantum yield of fluorescence. These spectral changes were not observed for pHLIP-C4phall or pHLIP-C6phall in the pH range of 6–8 (data not shown). We concluded that pHLIP-C10phall in solution at pH 6 is partially aggregated, which alters its interaction with the lipid bilayer of the cellular membrane and leads to a reduction of the antiproliferative effect.

DISCUSSION

In conventional drug design and discovery, the Lipinski rules of five, or subsequently developed similar parameters, are widely used to guide drug design. The rules postulate that a successful drug should be hydrophobic and small to traverse membranes and reach cytoplasmic targets (e.g., the logarithm of the octanol–water partition coefficient, log *P*, is −0.4 to 5.6 and the molecular mass is 160–480 Da).[23] However, the majority of inhibitors found for biological targets located inside a cell are molecules that cannot cross a membrane.[24–26] We have proposed a novel way to deliver polar molecules across membranes, based on the insertion of a water-soluble, moderately hydrophobic membrane peptide, pHLIP. The spontaneous insertion and folding of the peptide into a lipid bilayer seek the free energy minimum, and the insertion event is therefore accompanied by a release of energy, which is used to translocate cell-impermeable cargo molecules across a cellular membrane. The Gibbs free energy of binding of pHLIP to a POPC surface at 37 °C is approximately −7 kcal/mol at pH 8, and the additional free energy of insertion and folding across a lipid bilayer induced by a reduction in the pH from 8 to 4 is nearly −2 kcal/mol.[13] The energy difference between membrane-bound and membrane-inserted states favors the partition of cargo across the hydrophobic barrier of a membrane. Because the energy released during peptide folding and insertion across a membrane is limited and strongly polar molecules will reach equilibrium slowly, we assumed that there is a limit on the polarity of cargo (and most probably on size as well) that can be delivered across a membrane by pHLIP. In support of that, we recently showed that pHLIP can move phalloidin across a membrane to inhibit cell proliferation, but only when a hydrophobic facilitator (rhodamine) is attached to the peptide inserting end. In this study, we made a first attempt to tune the hydrophobicity of polar cargo phallacidin in a systematic manner by conjugation of phallacidin with diamines with different hydrophobic chain lengths. The hydrophobicity of the cargo is modulated by presence of 4–10 carbon atoms conjugated to the carboxyl group of phallacidin. The cargoes were synthesized and characterized. We show that the logarithm of the octanol–water partition coefficient (log *P*) of cargoes was varied from −1.6 for pure phallacidin to 1.28 for phallC10. Cargo, to be functional, needs to bind to its cellular target; in the case of phallacidin, it is F-actin. We evaluated the actin binding ability of cargoes and demonstrated that attachment of a chain of carbon atoms (up to 10 atoms) to the carboxyl group of phallacidin does not affect the ability of the cargo to interact with F-actin. Next, the phallC_n cargoes were conjugated via a

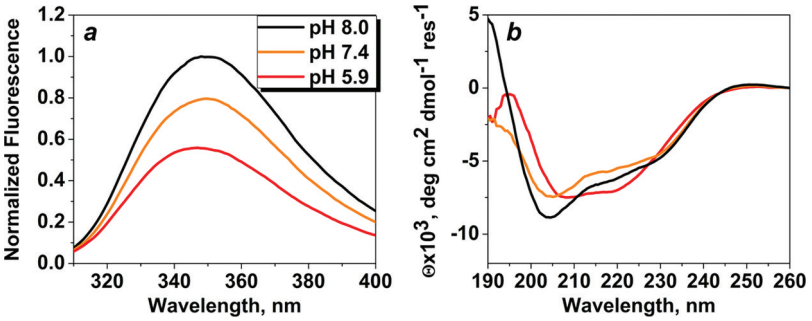

Figure 5. Intrinsic peptide fluorescence (a) and CD (b) spectral signals of pHLIP-C10phall at various pH values.

dx.doi.org/10.1021/bi2009773 | *Biochemistry* 2011, 50, 10215–10222

cleavable S−S bond to the C-terminus of pHLIP, which traverses the membrane. First, we spectroscopically characterized pHLIP-$C_n$phall cargoes. The experiments were conducted on a model system of POPC liposomes. The constructs, first, were dissolved in aqueous solution at pH 8 and then preincubated with liposomes at pH 8, and after that, the pH was decreased from 8 to 4. The conditions of the model experiment differ from the conditions of the experiments with cultured cells, while the conditions were chosen to ensure completion of all transitions and for the comparison to our previously published biophysical studies.[4−13] In general, we observed characteristic changes in the fluorescence and CD signals, when pHLIP-$C_n$phall interacts with the lipid bilayer of a POPC membrane at neutral and low pH values, as observed for pHLIP peptide.[4−13] The changes in the spectroscopic signals were the most pronounced for pHLIP-C10phall compared to pHLIP-C4phall. It was an important sign, indicating that attachment of phallC_n cargo molecules to the inserting end of the peptide does not prevent pH-dependent membrane interaction of the peptide. Next, we conducted cell experiments to demonstrate that phallC_n could be translocated across a membrane by pHLIP to induce inhibition of cell proliferation. It is known that phallacidin in the cytoplasm stabilizes actin in its filamentous form, preventing depolymerization. Because cell movement and shape changes are associated with actin polymerization and depolymerisation, stabilization of F-actin depolymerization leads to the freezing of cell movement, formation of multinucleated cells, and eventually cell death.[8,20] Phallacidin and phallC_n did not have any biological effect at either pH, while pHLIP facilitated translocation of phallC4 and phallC6 cargoes at slightly acidic pH, which in turn led to the inhibition of cell proliferation in a concentration-dependent manner. As we expected, the antiproliferative effect was more significant in the case of cell treatment with pHLIP-C6phall than with pHLIP-C4phall, because phallC6 is more hydrophobic than phallC4. However, surprisingly, we did not monitor the desired biological effect when cells were treated with pHLIP-C10phall. Additional characterization of the conformational states of pHLIP-C10phall in aqueous solutions in the pH range of 6−8 revealed that the construct has a much stronger tendency to aggregate at pH 6 (pH used to treat cells) compared to the tendencies of pHLIP, pHLIP-C4phall, and pHLIP-C6phall. As a result, the efficacy of treatment was reduced. We concluded that an increase of cargo hydrophobicity indeed facilitates its translocation across a membrane by pHLIP; however, the requirement of construct solubility is critical, because interaction of the construct with the cell membrane could be altered, leading to the weakened translocation ability and diminished biological effect.

In contrast to all other known peptide-based delivery technologies, selective delivery of molecules into the cytoplasm by pHLIP is achieved by the pH-dependent folding of a monomeric peptide across the plasma membrane. In response to the low extracellular pH values of cells in diseased tissues, pHLIP can translocate polar therapeutic cargo molecules into cell cytoplasms, whereas at the normal extracellular pH of healthy tissue, only a minimal translocation of cargo across cell membranes would occur. Because the cargo is translocated across a cell membrane directly into the cytoplasm, endosomal trapping is avoided. Tuning the cargo hydrophobicity can be used to achieve the maximal difference between the therapeutic effect at low pH versus neutral pH, thereby enhancing disease-targeted delivery and reducing treatment side effects. However, to achieve the desired enhancement of therapeutic efficacy, it is critical to ensure the solubility of the construct, which could be reduced because of the increase in cargo hydrophobicity.

AUTHOR INFORMATION

Corresponding Author

*Physics Department, University of Rhode Island, 2 Lippitt Rd., Kingston, RI 02881. Phone: (401) 874-2060. Fax: (401) 874-2380. E-mail: reshetnyak@mail.uri.edu.

Funding

This work was supported by National Institutes of Health Grant CA133890 to O.A.A., D.M.E., Y.K.R. and U.S. Department of Defense Grant PC050351 to Y.K.R.

ACKNOWLEDGMENTS

We thank Dr. Anna Moshnikova and Erin Jansen (Physics Department, University of Rhode Island) for help with cell experiments and purification of constructs, respectively; Prof. Brenton DeBoef and Dr. Shathaverdhan Potavathri (Chemistry Department, University of Rhode Island) for guidance in phallacidin cargo synthesis; and Dr. Ming An (Department of Molecular Biophysics and Biochemistry, Yale University) and Dr. Gregory Watkins (Delpor, Inc.) for discussion.

REFERENCES

(1) Jeffrey, S. S., Lonning, P. E., and Hillner, B. E. (2005) Genomics-based prognosis and therapeutic prediction in breast cancer. *J. Natl. Compr. Cancer Network 3*, 291−300.

(2) Krebs, H. A. (1972) The Pasteur effect and the relations between respiration and fermentation. *Essays Biochem. 8*, 1−34.

(3) Warburg, O., Wind, F., and Negelein, E. (1927) The metabolism of tumors in the body. *J. Gen. Physiol. 8*, 519−530.

(4) Hunt, J. F., Rath, P., Rothschild, K. J., and Engelman, D. M. (1997) Spontaneous, pH-dependent membrane insertion of a transbilayer α-helix. *Biochemistry 36*, 15177−15192.

(5) Reshetnyak, Y. K., Segala, M., Andreev, O. A., and Engelman, D. M. (2007) A monomeric membrane peptide that lives in three worlds: In solution, attached to, and inserted across lipid bilayers. *Biophys. J. 93*, 2363−2372.

(6) Andreev, O. A., Engelman, D. M., and Reshetnyak, Y. K. (2009) Targeting acidic diseased tissue: New technology based on use of the pH (Low) Insertion Peptide (pHLIP). *Chem. Today 27*, 34−37.

(7) Andreev, O. A., Engelman, D. M., and Reshetnyak, Y. K. (2010) pH-sensitive membrane peptides (pHLIPs) as a novel class of delivery agents. *Mol. Membr. Biol. 27*, 341−352.

(8) Reshetnyak, Y. K., Andreev, O. A., Lehnert, U., and Engelman, D. M. (2006) Translocation of molecules into cells by pH-dependent insertion of a transmembrane helix. *Proc. Natl. Acad. Sci. U.S.A. 103*, 6460−6465.

(9) Thevenin, D., An, M., and Engelman, D. M. (2009) pHLIP-mediated translocation of membrane-impermeable molecules into cells. *Chem. Biol. 16*, 754−762.

(10) Andreev, O. A., Dupuy, A. D., Segala, M., Sandugu, S., Serra, D. A., Chichester, C. O., Engelman, D. M., and Reshetnyak, Y. K. (2007) Mechanism and uses of a membrane peptide that targets tumors and other acidic tissues in vivo. *Proc. Natl. Acad. Sci. U.S.A. 104*, 7893−7898.

(11) Musial-Siwek, M., Karabadzhak, A., Andreev, O. A., Reshetnyak, Y. K., and Engelman, D. M. (2010) Tuning the insertion properties of pHLIP. *Biochim. Biophys. Acta 1798*, 1041−1046.

(12) Barrera, F. N., Weerakkody, D., Anderson, M., Andreev, O. A., Reshetnyak, Y. K., and Engelman, D. M. (2011) Roles of Carboxyl Groups in the Transmembrane Insertion of Peptides. *J. Mol. Biol. 413*, 359−371.

(13) Reshetnyak, Y. K., Andreev, O. A., Segala, M., Markin, V. S., and Engelman, D. M. (2008) Energetics of peptide (pHLIP) binding to

and folding across a lipid bilayer membrane. *Proc. Natl. Acad. Sci. U.S.A. 105*, 15340−15345.
(14) Andreev, O. A., Karabadzhak, A. G., Weerakkody, D., Andreev, G. O., Engelman, D. M., and Reshetnyak, Y. K. (2010) pH (low) insertion peptide (pHLIP) inserts across a lipid bilayer as a helix and exits by a different path. *Proc. Natl. Acad. Sci. U.S.A. 107*, 4081−4086.
(15) Tang, J., and Gai, F. (2008) Dissecting the membrane binding and insertion kinetics of a pHLIP peptide. *Biochemistry 47*, 8250−8252.
(16) Vavere, A. L., Biddlecombe, G. B., Spees, W. M., Garbow, J. R., Wijesinghe, D., Andreev, O. A., Engelman, D. M., Reshetnyak, Y. K., and Lewis, J. S. (2009) A novel technology for the imaging of acidic prostate tumors by positron emission tomography. *Cancer Res. 69*, 4510−4516.
(17) Reshetnyak, Y. K., Yao, L., Zheng, S., Kuznetsov, S., Engelman, D. M., and Andreev, O. A. (2010) Measuring Tumor Aggressiveness and Targeting Metastatic Lesions with Fluorescent pHLIP. *Mol. Imaging Biol.*, DOI: doi: 10.1007/s11307-010-0457-z.
(18) Wieland, T. (1977) Modification of actins by phallotoxins. *Naturwissenschaften 64*, 303−309.
(19) Barak, L. S., and Yocum, R. R. (1981) 7-Nitrobenz-2-oxa-1,3-diazole (NBD)-phallacidin: Synthesis of a fluorescent actin probe. *Anal. Biochem. 110*, 31−38.
(20) An, M., Wijesinghe, D., Andreev, O. A., Reshetnyak, Y. K., and Engelman, D. M. (2010) pH-(low)-insertion-peptide (pHLIP) translocation of membrane impermeable phalloidin toxin inhibits cancer cell proliferation. *Proc. Natl. Acad. Sci. U.S.A. 107*, 20246−20250.
(21) Wieland, T., Hollosi, M., and Nassal, M. (1983) Components of the green deathcap mushroom (*Amanita phalloides*), LXI: delta-Aminophalloin, a 7-analogue of phalloidin, and some biochemically useful, including fluorescent derivatives. *Liebigs Ann. Chem. 1983*, 1533−1540.
(22) Falcigno, L., Costantini, S., D'Auria, G., Bruno, B. M., Zobeley, S., Zanotti, G., and Paolillo, L. (2001) Phalloidin synthetic analogues: Structural requirements in the interation with F-actin. *Chem.—Eur. J. 7*, 4665−4673.
(23) Lipinski, C. A., Lombardo, F., Dominy, B. W., and Feeney, P. J. (2001) Experimental and computational approaches to estimate solubility and permeability in drug discovery and development settings. *Adv. Drug Delivery Rev. 46*, 3−26.
(24) Tsutsumi, S., and Neckers, L. (2007) Extracellular heat shock protein 90: A role for a molecular chaperone in cell motility and cancer metastasis. *Cancer Sci. 98*, 1536−1539.
(25) Wang, J. L., Zhang, Z. J., Choksi, S., Shan, S., Lu, Z., Croce, C. M., Alnemri, E. S., Korngold, R., and Huang, Z. (2000) Cell permeable Bcl-2 binding peptides: A chemical approach to apoptosis induction in tumor cells. *Cancer Res. 60*, 1498−1502.
(26) Sun, H., Nikolovska-Coleska, Z., Yang, C. Y., Qian, D., Lu, J., Qiu, S., Bai, L., Peng, Y., Cai, Q., and Wang, S. (2008) Design of small-molecule peptidic and nonpeptidic Smac mimetics. *Acc. Chem. Res. 41*, 1264−1277.